Prediction of Mechanical Properties of Hybrid FRP Composite for Out-of Plane Transverse Loading Using Micro Mechanical Approach

E. Kavitha 1, Dr.K.Sivaji Babu2, Dr M.R.S. Satyanarayana3 , Dr.V.Balakrishna Murthy4

1Assistant Professor, Department of Mechanical Engineering, PVP Siddhartha Institute of Technology, Vijayawada - 520010, India
Email.id - kavithavarikola@gmail.com Mobile: 9848309619
2 Professor, Department of Mechanical Engineering, PVP Siddhartha Institute of Technology, Kanuru, Vijayawada - 520010. , India
Email.id – k_sivajibabu@yahoo.com Mobile: 9490958212
3Professor, Department of Mechanical Engineering, GITAM University, Visakhapatnam - 045 - 530045, India
Email.id – rssmunukurthi@yahoo.com Mobile: 9493637939
4 Professor, Department of Mechanical Engineering, V.R.Siddhartha Engineering College, Kanuru, Vijayawada - 520010, India.
Email.id – vbkm64@yahoo.co.in

Abstract— The present research problem deals with the micromechanical analysis of a unidirectional continuous hybrid fiber-reinforced composite lamina. Three-dimensional models along with governing boundary conditions have been developed from the Representative Volume Elements (RVE) which are idealized as an array of square unit cells. The stress-strain relation in the finite element models takes place according to three-dimensional elasticity theory. The hybrid lamina consists of two different fibers of T-300 and S-GLASS materials, and epoxy matrix. The micromechanical analysis includes the evaluation of mechanical properties of the hybrid lamina at the fiber-matrix interface for perfectly bonded interfaces. In this phase of the work, the out-of-plane transverse Young's modulus (E3), Poisson's ratios (v31 and v32) are determined for a hybrid lamina for different volume fractions of fibers. In this case, the lamina is subjected to uniform pressure load in the out-of-plane transverse direction of the composite lamina and no debond is considered at the fiber-matrix interfaces.

Index Terms— Unit Cell, Finite Element Method, Hybrid Lamina

1 INTRODUCTION

In the recent period, there has been a tremendous advancement in the science and technology of fiber-reinforced composite materials. The low density, high strength, high stiffness to weight ratio, excellent durability and design flexibility of fiber-reinforced composites are the primary reasons for their use in many structural components, in aircraft, automotive, marine and other industries. Fiber-reinforced composites are now used in applications ranging from spacecraft frames to ladder rails, from aircraft wings to automobile doors, from rocket motor cases to oxygen tanks and from printed circuit boards to tennis rackets. Their use is increasing at such a rapid rate that they are no longer considered advanced exotic materials. The essence of fiber-reinforced composite technology is the ability to bond together of strong stiff fibers in the right place in the right orientation and right volume fraction. Fiber-reinforced composite materials consist of 'fibers' of high strength and modulus embedded in or bonded to a 'weak matrix', with distinct interface (boundary) between them. In this form, both fibers and matrix retain their physical and chemical identities, yet they produce a combination of properties that cannot be achieved with either of the constituents acting alone. In general, fibers are the principal load carrying members, while the surrounding matrix keeps them in the desired location and orientation, acts as a load transfer medium between them and protects them from environmental damages caused by elevated temperatures, humidity, etc. Thus even though the fibers provide reinforcement for the matrix, the latter also serves a number of useful functions in a fiber-reinforced composite material.

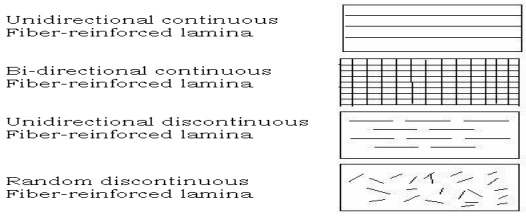

Fig. 1.1 Types of fiber-reinforcement

The fibers can be incorporated into a matrix either in continuous lengths or discontinuous forms (Fig. 1.1). The principal fibers in commercial use are various types of glass, carbon, Kevlar etc. fibers. Other fibers such as boron, silicon carbide, aluminum oxide are al-

so used in limited quantities. The matrix material may be a polymer, a metal, or a ceramic. Authors [1-4] have determined the elastic constants of FRP composites for various types of constituents. Takashi Ishiwaka et al [5] has conducted an experiment to obtain the elastic modulii of uni directional carbon FRP composites. Hashin, Z[6] has reviewed the analysis of FRP composite materials in the mechanical and materials point of view. Li, S. et al [7] has developed two idealized typical packing systems that have been employed for the unidirectional FRP composites in order to accommodate Fibers at irregular cross sections and imperfections. Morais, A. B. et al [8] predicted the properties and behavior of the composite which are influenced by the properties of fiber and matrix interfacial bond by its micro structure. Hyer, M. W. et al [10] got the expressions for E1 using the theory of elasticity approach. Sun et al [11] has developed representative volume element [RVE] to predict the mechanical properties of Uni directional Fiber composites. Peter Schwartz [12] experimentally investigated the fiber matrix interface properties by using single fiber pull out from a micro composite [SFPOM] test. Micromechanics are intended to study the distribution of stresses and strains within the micro regions of the composite under loading. This study will be particularized to simple loading and geometry for evaluating the average or global stiffness's and strength of the composites.

The results of micromechanics will help to understand load distribution, microscopic structure, comprehend the influence of microstructure on the properties of composite, predict the average properties of the lamina, and to design the materials, i.e., constituent and their distribution, for a given situation.

The properties and behavior of a composite are influenced by the properties of fiber and matrix, interfacial bond and by its microstructure. For a fiber of given cross-sectional shape, the size and quality of the surface directly influence the load transferring bond. The bond strength improves with the increase of ratio of surface area to the volume of reinforcement, for circular fibers of unit length and radius r, Surface area/volume=2/r. Hence the bond area increases with finer fibers.

Concept of unit cells-The distribution (or packing) of fibers in a plane normal to the axis of fibers is random (Fig.1.2). The analysis of any region of such a lamina is unwieldy. In order to tackle the problem by analytical tools, the microstructure of lamina is idealized. Idealization is done assuming that the fibers are straight and lay parallel to each other and that their distribution cross-section follows regular pattern as shown in Fig1.3. The typical fiber packing pattern used for the lamina structural idealization is staggered square array (Fig. 1.3)

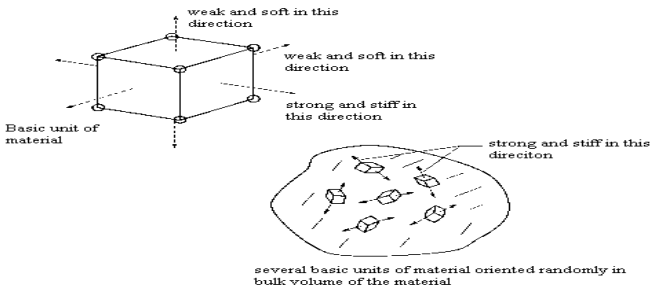

Fig. 1.2 Basic unit of a material

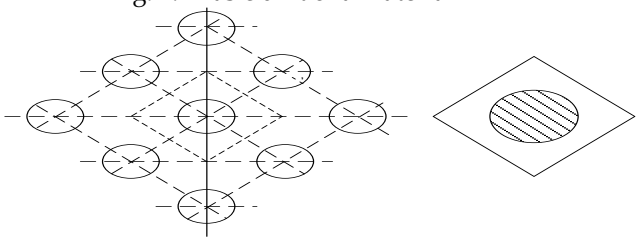

Fig. 1.3 Staggered Square array of circular fibers and representative volume element

2.EXPERIMENTAL PROCEDURE

Micromechanical behavior of the unidirectional continuous hybrid fiber-reinforced composite lamina subjected to out of plane transverse loading is discussed. A three-dimensional finite element model has been developed from the unit cells of staggered square pattern of the composite to predict the out-of-plane transverse Young's moduli (E_3) and corresponding Poisson's ratios (v_{31} and v_{32}) of a hybrid fiber-reinforced lamina with combination of T300 and S-glass materials for various volume fractions. The finite element software ANSYS has been successfully executed to evaluate the properties at different volume fractions.

3. METHODOLOGY

The unidirectional continuous fiber reinforced composite lamina has been idealized as a large array of representative volume elements. Depending upon the arrangement of the fibers across the cross section of the lamina, different types of representative volume elements can be obtained such as square, hexagonal, staggered square patterns etc. In any pattern repetition of a particular volume of the lamina can be observed, which is called the representative volume element (RVE) or unit cell.

For the present analysis, the lamina is considered as an array of staggered square unit cells (Fig. 3.1) and one unit cell is adopted for the micromechanical analysis of the lamina. For the present problem, the unit cell is considered as a prism

of square cross section embedded with four quarter cylinders at the four corners of the unit cell. This type of square unit cell is adopted in order to accommodate fibers of two different materials arranged in alternate rows. The cross sectional area of the fibers in the unit cell is governed by the fiber volume fraction, which is the ratio of the volume of the fiber to the total volume of the unit cell.

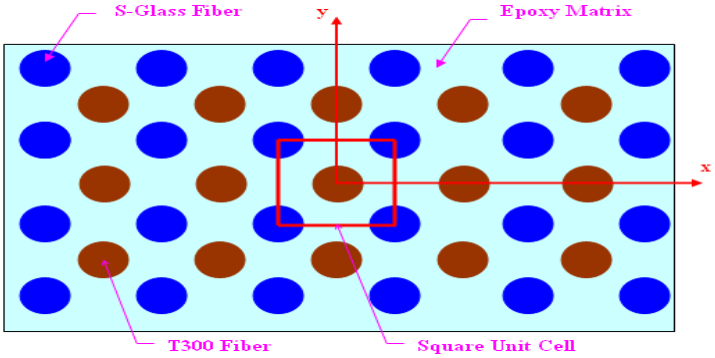

Fig. 3.1 Hybrid composite lamina

3.2.1 Loading

Uniform tensile load of 1 MPa is applied in the in-plane transverse direction (along 2- or x- axis) on the area at X=100 units.

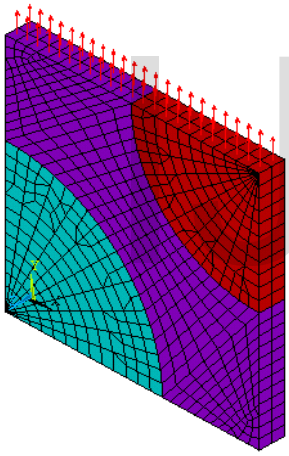

Fig. 3.2 Finite Element mesh showing out-of-plane transverse load on one-eighth portion of the unit cell

3.2.2 Boundary conditions

Due to the symmetry of the problem, the following symmetric boundary conditions are used

- On the surface at x=0, Ux=0
- On the surface at y=-100, Uy=0
- On the surface at z=0, Uz=0

In addition the following multi-point constraints are used.

The Ux of all the nodes on the area at x=100 is same
The Uy of all the nodes on the area at y=100 is same
The Uz of all the nodes on the area at z=10 is same

3.3 RESULTS

The mechanical properties of the lamina are calculated using the following expressions.

Young's modulus in fiber direction

$$E_3 = \sigma_3/\varepsilon_3$$

Poisson's Ratio $\nu_{31} = -\varepsilon_1/\varepsilon_3$

$$\nu_{32} = -\varepsilon_2/\varepsilon_3$$

Where

σ_1=Stress in 1-direction (z-direction).
ε_1=Strain in 1-direction (z-direction)=displacement of the FE model in z-direction/10)
ε_2=Strain in 2-direction (x-direction)=displacement of the FE model in x-direction/100)
ε_3=Strain in 3-direction (y-direction)=displacement of the FE model in y-direction/100)

Sufficient numbers of convergence tests are made and the present finite element model is validated by comparing the Young's modulus of T300-Epoxy lamina predicted with the value obtained from exact elasticity theory (102) and found close agreement .Later the finite element model is used to evaluate the properties E_3, ν_{31}, ν_{32} of a hybrid composite with T300 and Sglass fibers. Figs below presents the mechanical properties predicted from the present analysis for different combinations of volume fractions.

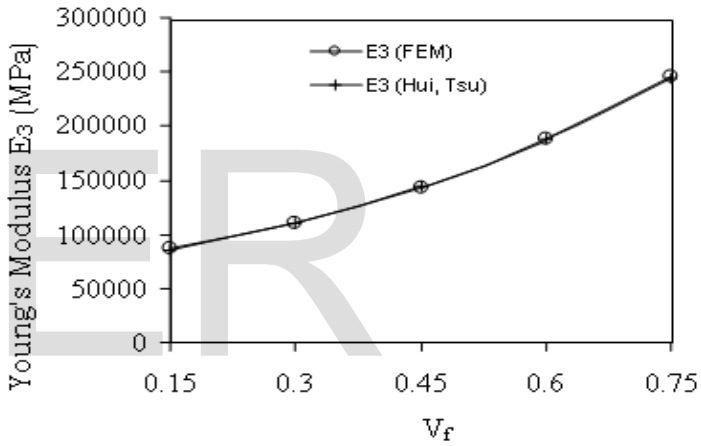

Fig. 3.3 Validation of present FE model for E_3

3.4 ANALYSIS OF RESULTS

3.4.1 Variation of E_3 with respect to V_f:

It is observed that there is a linear increment of the young's modulus with respect to volume fraction for all the three combinations up to V_f=30%. For V_f from 30% to 60% the young's modulus increases at a slow rate. For V_f between 60% and 70% it increases at a faster rate for S-glass T300 epoxy and hybrid epoxy composites. This is because the stiffness of the composite increases with increase in volume fraction (V_f). The young's modulus of S-glass epoxy at all the volume fractions is observed to be maximum followed by hybrid-epoxy and T300-epoxy, due to the less value of T300 fiber transverse modulus when compared with S-glass fiber modulus.

M1= T300 EPOXY: M2 = HYBRID EPOXY: M3 = SGLASS EPOXY

Fig.3.4 Variation

Fig 3.4: Variation of E_3 with respect to V_f

3.4.2 Variation of Poisson's Ratio (v_{31}) with respect to V_f:

The Poisson's Ratios (v_{31}) decreases from V_F =10% to 50% , and later increases for S-glass. For T300 epoxy and hybrid epoxy it shows a decreasing trend throughout.

M1= T300 EPOXY: M2 = HYBRID EPOXY: M3 = SGLASS EPOXY

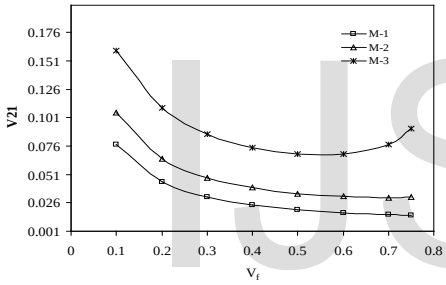

Fig 3.5: Variation of v_{31} with respect to V_f

3.4.3 Variation of Poisson's Ratio (v_{32}) with respect to V_f:

The Poisson's Ratios (v_{32}) gradually decreases with increase in volume fractions for T300 and hybrid epoxy. For S-glass it shows a increasing trend from V_f =10% to 60% and later increases the Poisson's ratio decreases at a slow rate.

M1= T300 EPOXY: M2 = HYBRID EPOXY: M3 = SGLASS EPOXY

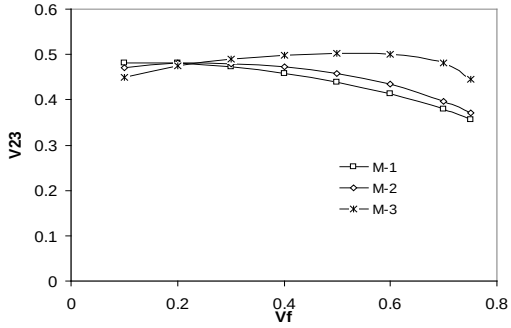

Fig 3.6: Variation of v_{32} with respect to V_f

3.4.4 Variation of Young's modulus (E_3) with respect to Non-uniform V_f:

(V_f for lower fiber is constant):

It is observed that there is a linear increment of the young's modulus with respect to volume fraction for all the three combinations up to V_f =30%. For V_f from 30% to 60% the young's modulus increases at a slow rate. For V_f between 60% and 70% it increases at a faster rate for S-glass epoxy and hybrid epoxy composites. This is because the stiffness of the composite increases with increase in volume fraction (V_f). The young's modulus of S-glass epoxy at all the volume fractions is observed to be maximum followed by hybrid-epoxy and T300-epoxy, due to the less value of T300 fiber transverse modulus when compared with S-glass fiber modulus.

M1= T300 EPOXY: M2 = HYBRID EPOXY: M3 = SGLASS EPOXY

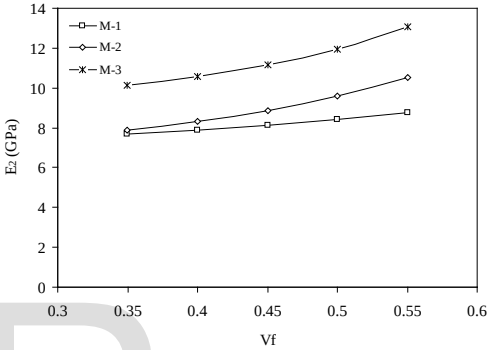

Fig 3.7: Variation of E_3 with respect to V_f

3.4.5 Variation of Poisson's Ratio (v_{31}) with respect to Non-uniform V_f:

The Poisson's Ratios (v_{31}) shows a decreasing trend throughout for S-glass epoxy and T300 with increase in volume fractions. For hybrid epoxy it is observed that the Poisson's ratio decreases from V_f =35% to 45% and later the Poisson's ratio increases at a slow rate. The Poisson's Ratio of S-glass epoxy at all the volume fractions is observed to be maximum followed by hybrid epoxy and T300 epoxy.

M1= T300 EPOXY: M2 = HYBRID EPOXY: M3 = SGLASS EPOXY

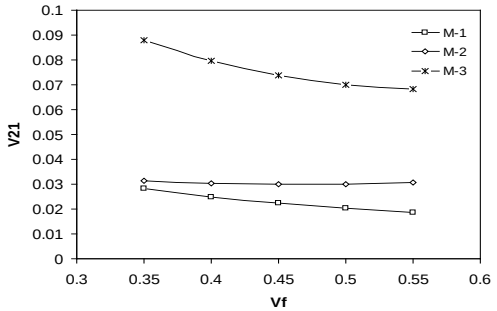

Fig 3.8: Variation of v_{31} with respect to V_f

3.4.6 Variation of Poisson's Ratio (v_{32}) with respect to Non-uniform V_f:

The Poisson's Ratios (v_{32}) shows a decreasing trend throughout for T300. For hybrid epoxy it is observed that the

Poisson's ratio increases from V_f =30% to 45% and later the Poisson's ratio decreases at a slow rate. The Poisson's Ratio of S-glass epoxy increases throughout at a faster rate.

M1= T300 EPOXY: M2 = HYBRID EPOXY: M3 = SGLASS EPOXY

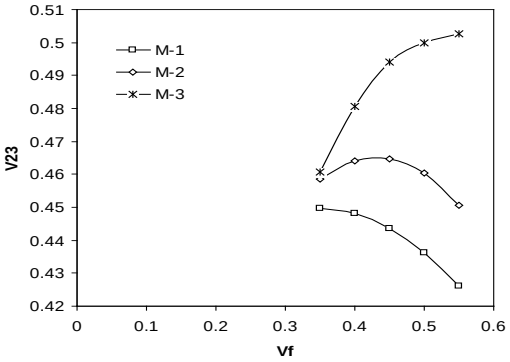

Fig 3.9: Variation of v_{32} with respect to V_f

3.4.6 Variation of Young's modulus (E_3) with respect to Non-uniformV_f

(V_f for upper fiber is constant)

It is observed that the young's modulus (E_3) increases with increase in the volume fraction (V_f)for all the three combinations. The young's modulus of S-glass epoxy at all the volume fractions is observed to be maximum followed by hybrid-epoxy and T300-epoxy, due to the less value of T300 fiber transverse modulus when compared with S-glass fiber modulus.

M1= T300 EPOXY: M2 = HYBRID EPOXY: M3 = SGLASS EPOXY

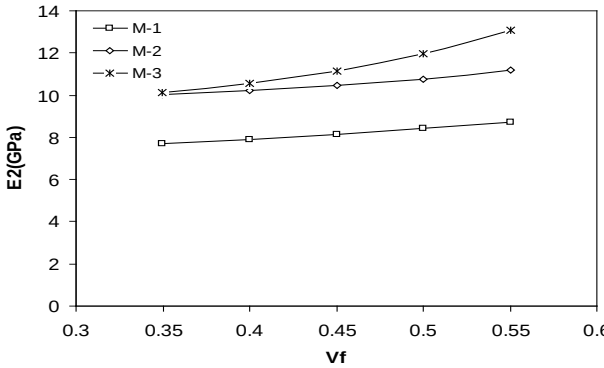

Fig 3.10: Variation of E_3 with respect to V_f

3.4.7 Variation of Poisson's Ratios (v_{31}) with respect to Non-uniform V_f:

The Poisson's Ratios (v_{31}) shows a decreasing trend throughout for all the three combinations. The young's modulus of S-glass epoxy at all the volume fractions is observed to be maximum followed by hybrid-epoxy and T300-epoxy

M1= T300 EPOXY: M2 = HYBRID EPOXY: M3 = SGLASS EPOXY

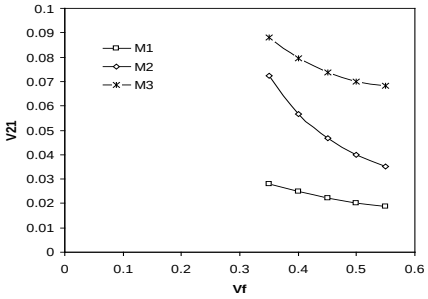

Fig 3.11: Variation of v_{31} with respect to V_f

3.4.8 Variation of Poisson's Ratios (v_{32}) with respect to Non-uniform V_f:

The Poisson's Ratios (v_{32}) shows a decreasing trend throughout for T300. For hybrid-epoxy it is observed that poisson's ratio increases from V_f =30% to 45% and later the Poisson's ratio decreases at a slow rate. The Poisson's Ratio of S-glass epoxy increases throughout at a faster rate.

M1= T300 EPOXY: M2 = HYBRID EPOXY: M3 = SGLASS EPOXY

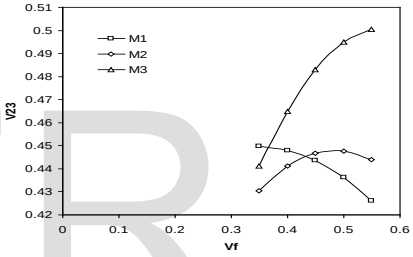

Fig 3.12: Variation of v_{32} with respect to V_f

3.4.9 Variation of Young's modulus (E_3) with respect to Non-uniform V_f

(V_f for various combinations)

When the volume fractions (V_f) of T300 fiber is increased and volume fractions (V_f) of S-glass fiber is decreased it is observed that the young's modulus (E_3) decreases at a slow rate and then increases for S-glass epoxy, T300 and for hybrid-epoxy the young's modulus (E_3) decreases throughout for various combinations. The young's modulus of S-glass epoxy at all the volume fractions is observed to be maximum.

M1= T300 EPOXY: M2 = HYBRID EPOXY: M3 = SGLASS EPOXY

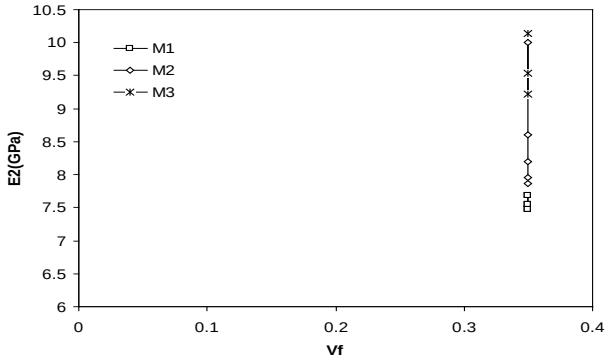

Fig 3.13: Variation of E_3 with respect to V_f

3.4.10 Variation of Poisson's Ratios (v_{31}) with respect to V_f: ▪ (V_f for various combinations)

When the volume fractions (V_f) of T300 fiber is increased and volume fractions (V_f) of S-glass fiber is decreased it is observed that the poisson's ratio(v_{31}) decreases at a slow rate and then increases for S-glass epoxy, T300 . For hybrid-epoxy the poisson's ratio decreases throughout for various combinations. The young's modulus of S-glass epoxy at all the volume fractions is observed to be maximum.

M1= T300 EPOXY: M2 = HYBRID EPOXY: M3 = SGLASS EPOXY

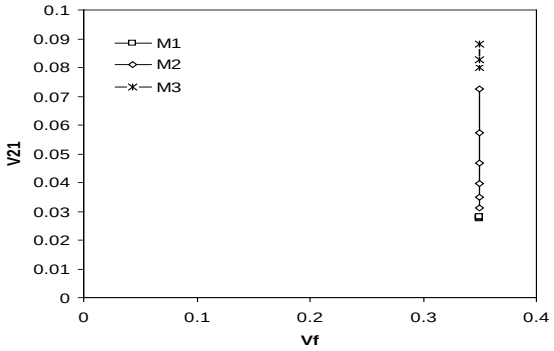

Fig 3.14: Variation of v_{31} with respect to V_f

3.4.11 Variation of Poisson's Ratios (v_{32}) with respect to V_f: (V_f for various combinations)

When the volume fractions (V_f) of T300 fiber is increased and volume fractions (V_f) of S-glass fiber is decreased it is observed that the poisson's ratio(v_{32}) decreases at a slow rate and then increases for all the three fibers.

M1= T300 EPOXY: M2 = HYBRID EPOXY: M3 = SGLASS EPOXY

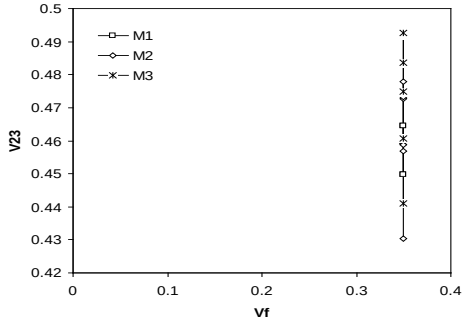

Fig 3.15: Variation of v_{32} with respect to V_f

4. CONCLUSIONS

The micromechanical behavior of hybrid FRP lamina for in plane transverse loading has been studied using finite element method. The Young's modulus (E_3) and Poisson's ratios (v_{31} and v_{32}) are predicted for different fiber volume fractions. The following conclusions are drawn.

- The Young's modulus is found to be increasing with V_f indicating that the stiffness of the composite increases with V_f .
- The Poisson's ratio (v_{32}) decreases with the increase in volume fraction for all the three combinations.

The Young's modulus is observed to be maximum for S-glass epoxy at volume fractions since in the out-of-plane transverse direction the E_3 transverse properties are more for S-glass.

REFERENCES

[1] Chen, C.H. and Cheng, S., 'Mechanical Properties of Anisotropic Fiber-Reinforced Composites', Trans. ASME J. of Applied Mechanics, vol. 37, no.1, 1970, p186-189.
[2] Hashin, Z. and Rosen B.W. 'The Elastic Modulii of Fiber–Reinforced Materials', Trans. ASME J. of Applied Mechanics ,vol.31, 1964, p223-232.
[3] Whitney, J.M., 'Elastic Modulii of Unidirectional Composites with anisotropic Filaments', J. of Comp. Materials, vol.1, 1967, p188-193.
[4] Hashin, Z., 'Analysis of Properties of Fiber Composites with anisotropic constituents', Trans. ASME J. of Applied Mechanics, vol.46, 1979, p543-550.
[5] Takashi Ishiwaka, Koyama, K and Kobayashi, S., 'Elastic Modulii of Carbon – Epoxy Composites and Carbon fibers', J. of Composite Materials, vol.11, 1977, p332-344.
[6] Hashin, Z., 'Analysis of Composite Materials- A Survey', Trans. ASME J. of Applied Mechanics, vol.50, 1983, p481-505.
[7] Li, S., 'On the unit cell for micromechanical analysis of fiber reinforced composites', Proc. R Soc. London A, 1999, p.815-838.
[8] Morais, A. B., 'Transverse modulii of continuous-fiber-reinforced polymers', Composites Science and Technology, vol.60, 2000, p.997-1002.
[9] ANSYS Reference Manuals (2006)
[10] Hyer, M. W., 'Stress Analysis of Fiber-Reinforced Composite Materials', McGraw-HILL Int., edition, 1998.
[11] Sun C T and Vaidya R S [1996] "prediction of composite properties from a representative volume element", composites science and technology, 56,pp 171-179.
[12] Yipping qiu, Peter Schwartz, composites science and technology, 47 [1993],pp 289-301.